



Detection, description, and technological properties of colour aberration in wood of standards and shoots from a chestnut (*Castanea sativa* Mill.) coppice stand

Swati Tamantini¹ · Sara Bergamasco¹ · Luigi Portoghesi¹ · Anna Maria Vettraino¹ · Florian Zikeli^{1,2} · Giuseppe Scarascia Mugnozza¹ · Manuela Romagnoli¹

Received: 18 November 2021 / Revised: 23 May 2022 / Accepted: 26 May 2022 / Published online: 24 June 2022

© The Author(s), under exclusive licence to Springer-Verlag GmbH Germany, part of Springer Nature 2022

Abstract

Sweet chestnut forests occupy an important role in Italy and Europe, its resilience is often affected by aggressive pathogen attack. In the last times some chestnut wood colour aberrations have attracted attention suggesting intercorrelation with biotic attacks. The present study analyses chestnut wood from a coppice-with-standards stand in Central Italy aiming to understand the reasons for discolorations in respect to a possible effect on wood physical and mechanical character. Wood specimens with different chromatic aberrations were analysed by mechanical tests, microscopic techniques (SEM), specific density measurements, and ATR-FTIR spectroscopy. Standing trees and logs were investigated by IML-RESI. Results by SEM show as all stained wood zones correspond to mycelium presence and abnormal cell wall morphologies. No real trend was found between specific density, or compressive strength, with coloured samples, infact some test samples with colour aberrations had the highest value for specific gravity. Comparing sound wood with stained wood, the semiquantitative analysis by ATR-FTIR spectroscopy allowed to detect a change in the ratio lignin/cellulose which might be due to a white rot fungus. IML-Resi has showed wood decay symptoms at root collar in coppice standards with a decrease in amplitude at least of 30%. The results find an agreement with similar studies carried out in Spanish chestnut suggesting to indeed the analysis to investigated the geographical distribution and the impact of the damage.

Keywords Wood decay · Compression strength · FTIR · SEM · Chestnut red stain · Forest decline

Introduction

Sweet chestnut (*Castanea sativa* Mill.) forests have an important ecological, social and economic role in Italy and in Central-Southern Europe. In Italy, the coverage throughout the country (800,000 ha) corresponds to nearly 2.6% of the total land area and 7.5% of the national forest area, respectively. In Europe, the species covers an area of 2.53 million ha (Conedera et al. 2016), which is 1.2% of the total

EU forest area. In Italy, chestnut forests are managed mainly as coppice stands (589,362 ha) or high forests intended both for chestnuts (15,506 ha) and timber production (147,568 ha) (Manetti et al. 2017).

Sweet chestnut forests and its wood have been the object of intensive research involving studies related to the identification of the most suitable forest management strategies (Manetti et al. 2017), wood quality studies (Romagnoli and Spina 2013; Spina and Romagnoli 2010), analysis of the chestnut-wood supply and value chain (Marini et al. 2021b) and studies to promote chestnut wood utilization in biobuilding (Brunetti et al. 2020; Carbone et al. 2020). Chestnut wood is always a hot topic for research not only to defend and promote the supply chain, which is one of the most important in certain regions (Marini et al. 2021b), but also because it was highlighted as one of the most promising species in the perspective of climate change impacts (Marini et al. 2019, 2021a) because of its origin in the climate of Southern Europe, which is the expected climate of

Communicated by Hans Pretzsch.

✉ Manuela Romagnoli
mroma@unitus.it

¹ Department for Innovation in Biological, Agro-Food and Forest Systems (DIBAF), University of Tuscia (UNITUS), Viterbo, Italy

² TU Wien, Institute of Chemical, Environmental and Bioscience Engineering, Vienna, Austria

the Central Europe in the near future (Conedera et al. 2021). However, an effective resilience of the species to climatic changes is a concern (Conedera et al. 2021; Freitas et al. 2021) due to its well-known sensitivity to abiotic and biotic threats, which can increase unpredictably causing difficulties to contain outbreaks (Bonsignore et al. 2020). Certain pathogens, for example, can reduce chestnut vitality and can cause important forest losses (Ferracini et al. 2019; Palmeri et al. 2014; Ugolini et al. 2014). Among the most destructive diseases of *Castanea* spp., there are *Phytophthora cambivora* (Petri) Buisman and *P. cinnamomi* Rands, agents of the chestnut ink disease, the ascomycete *Cryphonectria parasitica* (Murrill) M.E. Barr causing chestnut blight epidemic and the Asian gall wasp *Dryocosmus kuriphilus* Yasumatsu (Rigling and Prospero 2018; Sartor et al. 2015; Vannini et al. 2018; Vettrano et al. 2005). Those diseases can appear simultaneously on a single tree, multiplying the stress for the plant. Chestnut blight, for instance, can modify wood micromorphology and vessel frequency in synergy with the Asian chestnut gall wasp (Gunduz et al. (2016); Ugolini et al. (2014). In fact, vessel elements were proved to have a smaller diameter and a shorter length, moreover wood fibres had abnormal formation in comparison with healthy wood, such as bifurcation at the end of the cells (Gunduz et al. 2016). Chestnut is also affected by wood decay caused by several white and brown rot fungi (Beccaro et al. 2019). The basidiomycetes *Daedalea quercina*, *Fistulina hepatica* and *Laetiporus sulphureus* are the most widespread wood rot fungi attacking Chestnut. Beside that, it was also reported that extreme weather events may negatively affect tree health by increasing forest susceptibility to disease (Buotte et al. 2017), by enhancing the pests' growth and spreading and by weakening their enemies (Ayres and Lombardero 2000; Buotte et al. 2017; Pureswaran et al. 2018; Thurman et al. 2017). The strict and complex interaction between biotic and abiotic stresses renders difficult to understand the effect of a single stress factor. Several studies focused on the impact of climate changes on pathogens dynamics (Ayres and Lombardero 2000, Greco et al. 2018, Pureswaran et al. 2018). Blank et al. (2019) demonstrated that environmental conditions strongly influence the defoliation and dieback rate of *Pinus* spp. associated with *Fusarium circinatum* infections (Blank et al. 2019). All these factors cause physiological distress in plants usually reflecting on xylogenesis as well (Čufar et al. 2011; Romagnoli et al. 2011) which is characterized by a slower wood formation and narrower ring width (Camarero et al., 2018). In chestnut it is quite difficult to forecast how a slower growth reflects on ring width and, in consequence, on wood quality because the species is characterized by very large ring widths (Génova Fernández and Gracia Alonso 1984; Romagnoli et al. 2004). Indeed, the relationship between ring width and wood density, which is considered the main parameter associated with wood quality

is not linear (Romagnoli et al. 2014). Infact after threshold in ring width wood turns to have lower density and poorer physical properties than healthy wood (Camarero et al. 2018; Clair and Thibaut 2014; Militz et al. 2003). Camarero et al. (2018), showed as the species due to coppicing and very fast growth is not so much impacted in its ring width by defoliation (Camarero et al. 2018).

It is not the aim of this article to cover the wide-branched relationships between wood formation, ring width and wood quality which are affected by many parameters. This work aims to characterize chestnut wood from coppice stands affected by some pathogens where chromatic aberrations were observed. A physical (density, density profile by IML, wood colour measurement) and a chemical approach (FTIR spectroscopy) were used in order to understand if and how colour aberrations affect wood quality in terms of wood density and mechanical properties. The hypothesis is that we are assisting to a wood decay process, with a different level of degradation affecting at different extent wood tissues, located in stands showing signals of suffering.

Materials and methods

Study area and materials

The study was conducted on logs deriving from one of the most important chestnut wood production areas in the region of Lazio (Italy): Castelli Romani, where the soil is of volcanic origin. The sampling site for standing trees (G2 and G3) was at the municipality of Lariano (Colle Del Noce) at an altitude of 350 m a.s.l. and the selected area had a quite low slope. Climate data for the period 2004–2019 from the “Velletri” meteorological station (352 m a.s.l.; 41°41' N, 0°20' E) show an annual rainfall of 1300 mm and annual average temperature of 15 °C (max < 33 °C and min. > -2 °C). The investigated sampling site is managed as a coppice stand, the rotation period (T) is 24 years and the standards left standing have an age of 2 T (48 years). Chestnut stands are usually thinned at about 2/3 T (14–15 years). The forest coppice is monospecific (chestnut), but there are also several Turkey oaks (*Quercus cerris* L.) and pedunculate oaks (*Q. robur* L.) of large size. The medium diameter is 30 cm, and the medium height is 21.5 m. At the end of the rotation period, the total number of shoots per ha should be 1100–1200 with a mean trunk diameter at breast height of 40.9 cm (30.8 for shoots and 44.6 for standards). The reported yield is 250 m³/ha, summing up to a total yield of 5082 m³.

The sampling can be classified in three groups. The first sampling (G1) was conducted in October 2018 in a sawmill where some logs from stands in the Castelli Romani area were processed. In particular, the boles came from the area

located close to the investigated sites in Lariano municipality. Eight logs, all showing dark-brown coloured spots, were selected for further analysis to verify if the colour alteration could correspond to a loss of mechanical resistance by drilling method. The first sampling (G1) served the purpose of assessing the protocol to be used in the next on-site sampling. At that point, 2 disks per log were taken in order to perform the mechanical tests and, afterwards, the anatomical analyses by ATR-FTIR spectroscopy and SEM in representative specimens. A second sampling (G2) was carried out in April 2019 on the site Colle del Noce selecting 12 standing trees based on the observation of their physiological state, namely the crown dieback or intense epicormic branching. In fact, they presented epicormic branches although at a different extent. In the second group, the standing trees were investigated only with the drilling depth machine. The third group (G3) was selected in the same area of G1 and G2,

in October 2019 and the trees were investigated using the drilling depth machine as well. Further, it was possible to follow the complete transport chain from the forest site to the sawmill and finally, it was possible to take several disks (G3) as representative samples at about 50 cm from the bottom of the log.

Sampling methods, plants main characteristics and performed analyses are briefly explained in Table 1.

Detection of chromatic abnormalities and macroscopic inspection

Before starting the investigation of disks coming from sampling G1 and G3, macroscopic observation of the wood samples was carried out. The most important stain types are reported in Fig. 1 below. In Fig. 1a, there is an overview of stain types found in the specimens. Stains around the

Table 1 List of the selected trees and basic characteristics. Method of investigation applied are also reported

Group	ID	Class*	Diameter (cm)	Age	Notes
G1	G1-1	Standard	34,4	40	Analyses with IML-RESI in sawmill on logs. Mechanical tests (compression) and ATR-FTIR spectroscopy on test pieces. Anatomical analysis by SEM
	G1-2	Standard	50,8	42	
	G1-3	Standard	44,2	44	
	G1-4	Standard	42,8	74	
	G1-5	Standard	33,3	38	
	G1-6	Shoot	30,7	23	
	G1-7	Shoot	39,4	25	
	G1-8	Shoot	35,3	23	
G2	G2-1	Standard	29,9	–	Analyses with IML-RESI on standing trees
	G2-2	Standard	26,4	–	
	G2-3	Standard	28,7	–	
	G2-4	Standard	50,0	–	
	G2-5	Standard	57,3	–	
	G2-6	Standard	43,0	–	
	G2-7	Standard	37,6	–	
	G2-8	Shoot	27,4	–	
	G2-9	Shoot	22,0	–	
	G2-10	Shoot	25,5	–	
	G2-11	Shoot	39,2	–	
	G2-13	Shoot	29,9	–	
	G3	G3-1	Standard	60,5	
G3-2		Standard	72,0	38	
G3-3		Standard	80,3	45	
G3-4		Standard	55,7	44	
G3-5		Standard	45,9	38	
G3-6		Standard	20,7	48	
G3-7		Standard	33,4	48	

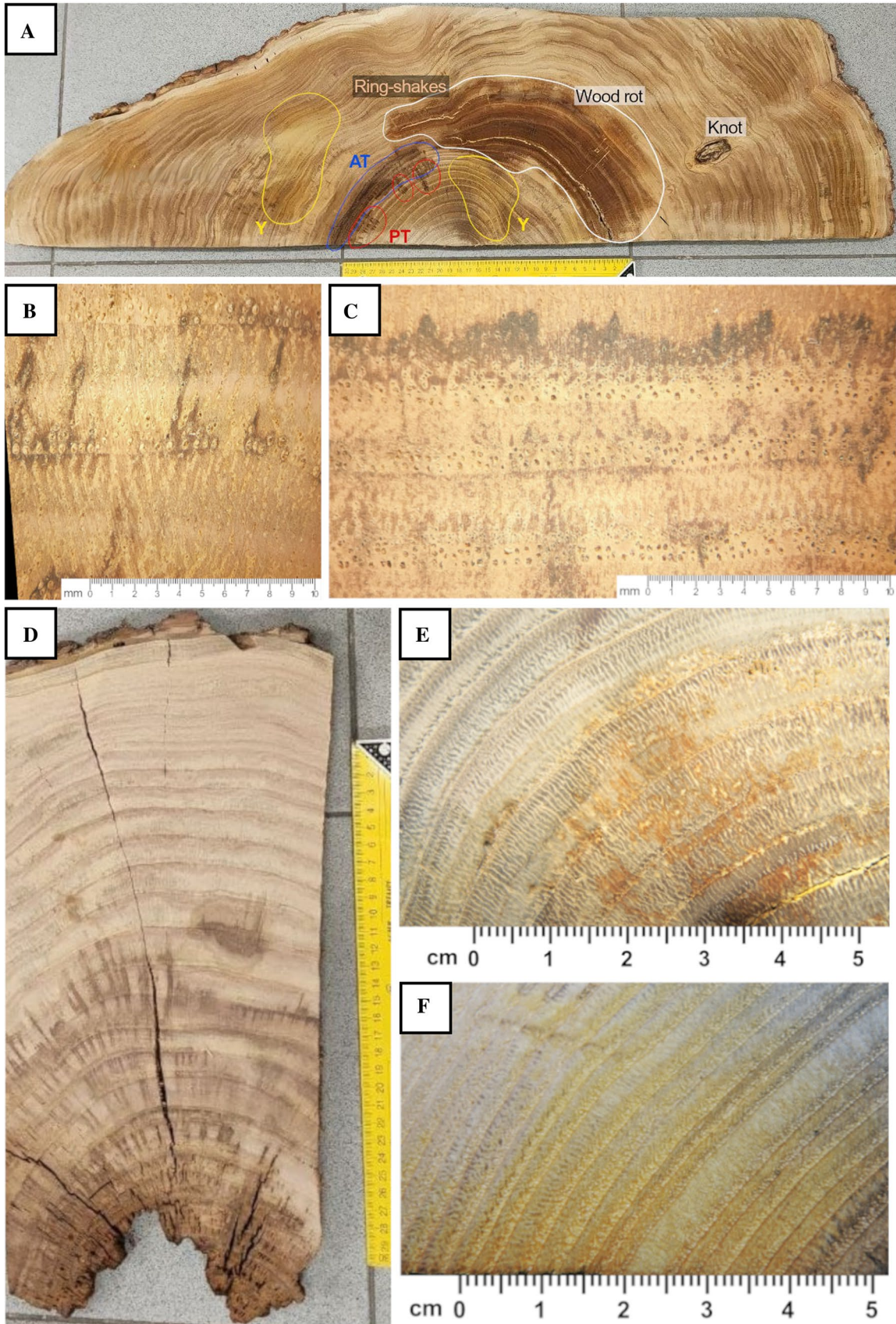


Fig. 1 **a** Overview of the stain types found in the specimens. **b** Paratracheal stains (PT). **c** Apotracheal stains (AT). **d** Type-A wood rot. **e** Type-B wood rot. **f** Yellow staining (Y)

vessels, hereinafter referred to as Paratracheal stains (PT), are shown in Fig. 1b. Similarly, stains spread throughout the ring (Fig. 1c) were hereinafter referred to as Apotracheal stains (AP). In Fig. 1d and e, there are two different type of wood rot, which were not previously identified, therefore, we named the first brownish stain Type-A wood rot and the second white-yellow colouration (Fig. 1e) Type-B wood rot. In Fig. 1f, a yellow area due to extractive accumulation (Y) is presented.

Drill resistance measurement

The inner conditions of wooden structures can be investigated by perforating the sample with a micro drilling machine (\varnothing 2 mm) (Costello and Quarles 1999; Imposa et al. 2014; Johnstone et al. 2007). In this study, an IML-RESI F400 drilling depth device (IML, Wiesloch, Germany) was used. Preliminary experiments were carried out in the sawmill: logs with presence of chromatic alterations were selected and one measurement at the bottom of the selected logs was taken. In the second and third sampling group (G2, G3), the analyses were carried out on standing trees, mainly at the diameter at breast high (DBH) or at the plant collar. The plants selected were rich of epicormic branching which was considered a plant response to damage or stress (Nicolini et al. 2003; Seybold et al. 2019). Density profiles were observed, it was assessed the healthy zone with mean amplitude in % was assessed. The degraded zone was assessed when an abrupt change in drilling was observed, the mean amplitude was later compared to the healthy zones.

Physical and mechanical characterization

Physical and mechanical tests were carried out on the disks taken from sampling G1 and G3. For each disk, samples were taken in radial direction from the pith to the bark, obtaining at average one to three specimens for each log depending on the original size of the cut disks.

The samples were conditioned at 12% moisture content (m.c.) and subsequently, the gravimetric density, the density at 12% m.c. (ρ_{12}) and stress in compression parallel to grain (σ_{12}) were measured, following the procedures described in Romagnoli and Spina (2013), Romagnoli et al. (2015), Romagnoli et al. (2014) and Marini et al. (2021a). Clear test samples measuring $20 \times 20 \times 30$ mm (R \times T \times L) were tested and measured. The universal testing machine Z050 (Zwick Roell, Ulm-Eisingen, Germany) was used with a pre-load

of 50 kN and an analysis speed of 5 mm/min according to the respective norm (UNI ISO 3787:1985).

Both wood density and mechanical properties were analysed paying attention to the stained areas previously described. Tests were carried out along the rays, starting from the piths until the sapwood border and the sapwood tissue was removed in the tested samples.

Spectroscopic analysis (ATR-FTIR spectroscopy)

One representative sample for each stain type was analysed with a Jasco IRT-7000 Irtron Infrared Microscope (Jasco Corporation, MD, USA) in the range of $2000\text{--}1000$ cm^{-1} , with 500 scans in absorbance mode, within an area of 100×100 μm . The analysis was carried out on the main selected chromatic aberrations illustrated in Fig. 1, selecting at least three different zones in the same colour patch area. IR bands were assigned according to Naumann et al. (2005), Özgenç et al. (2017) and Pandey and Pitman (2003).

Morphological and anatomical analysis (SEM)

After the ATR-FTIR analysis, the same samples were used for an anatomical morphological characterization by Scanning Electron Microscope analysis. The samples were attached to aluminium stubs by a carbon tape and sputter-coated with gold in a Balzers MED 010 unit (Oerlikon Balzers, Balzers, Liechtenstein). A JEOL JSM 6010LA SEM was used (JEOL Limited, Tokyo, Japan).

Results

In Table 2, the presence of colour aberrations is reported. In sampling group G1, half of the selected logs for the drilling depth measurements showed chromatic aberrations. In G3, following the chain from the forest to the sawmill, macroscopic observation identified 57% of the samples with evident signals of decay or chromatic aberration. It was noticed that all of the affected plants were standards.

Drill resistance measurement

The possibility to use a drill to detect wood decay is already known. Actually, the aim of this study, was not just to detect damaged wood, but rather to understand if the colour alterations correspond to damaged wood or if they are simply an extractive accumulation or other superficial phenomenon of wood alteration (i.e. oxidation) which has a different impact on cell wall integrity. Results show that wood with no colour aberration has a normal profile (Fig. 2a) without any abrupt change in density except at the ring transition from early-wood to latewood. In contrast, samples with visible colour

Table 2 Colour aberration presence in specimens

Group	ID	Class	Colour aberrations presence
G1	G1-1	Standard	✓
	G1-2	Standard	✓
	G1-3	Standard	✓
	G1-4	Standard	✓
	G1-5	Standard	
	G1-6	Shoot	
	G1-7	Shoot	
	G1-8	Shoot	
G3	G3-1	Standard	✓
	G3-2	Standard	
	G3-3	Standard	✓
	G3-4	Standard	
	G3-5	Standard	
	G3-6	Standard	✓
	G3-7	Standard	✓

alteration have a decrease in their respective density profile corresponding to the damage occurred (Fig. 2b).

In Fig. 2b, a gradual reduction in the density profile starting from the outer sound part towards the pith is evident corresponding to a strong sign of wood decay, drilling machine has detected a transition zone in the middle where it starts a gradual decrease.

Results of the drilling analyses in standing trees from groups G2 and G3 are less clear. All of the selected trees show phenotypic symptoms of suffering like epicormic

branches. For some samples, a regular drilling analysis profile was found (Fig. 3c), but it there is a possibility of a fungal attack at the collar of the tree, which is not yet visible at DBH (Fig. 3a and c). The analysis by drilling machine finds a confirmation when it was possible to investigate samples of the G3 groups (Fig. 3c). In the disks it was possible to observe signals of wood decay.

It was not possible to detect the presence of ring shakes in all samples. In fact, ring shake defects were observed only sometimes in cut trees, as it is known that this defect occurs occasionally after timber cutting and drying (Spina and Romagnoli 2010). Sometimes ring shakes are of traumatic origin and, thus, are associated with fungal infections through the scars. This leads to wood decay progression and consequently to a decrease in wood mechanical properties (Romagnoli and Spina 2013). Therefore, the detection of ring shakes can be important for an early detection of fungal attacks.

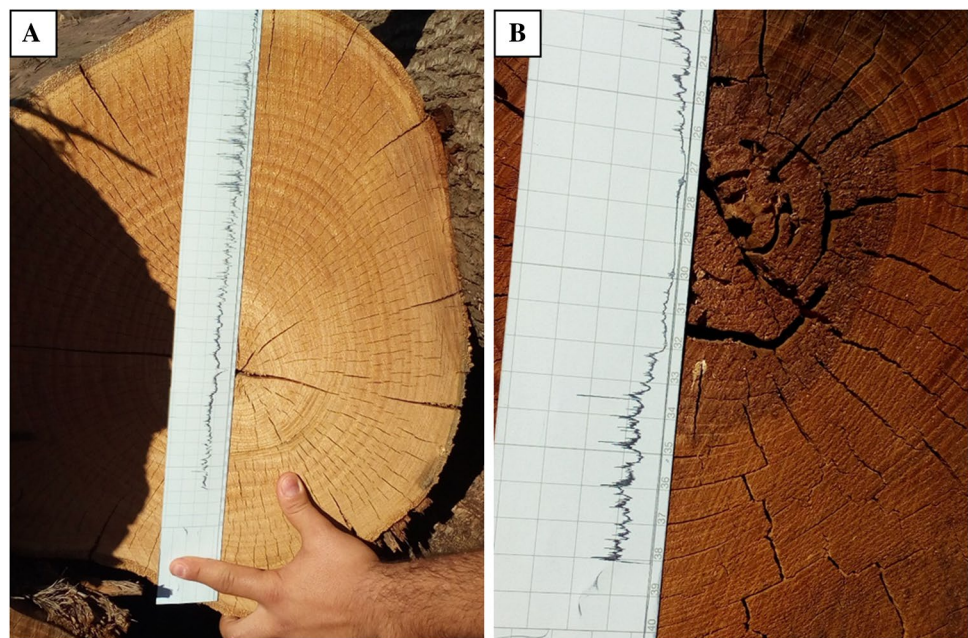
In Table 3, the amplitude of the estimated healthy and decayed zone of samples considered as decayed are reported together with the corresponding length of the density profile.

By Table 3, it is evident that when wood is considered decayed it is measured a decrease in amplitude which spans from about 30% (G1-7) up to 67% (G1-2).

Physical and mechanical characterization

In Table 4, results of density measurements and compression tests are shown. Specific density values groups are consistent with literature related to trees sampled in the area of Castelli Romani (0.500 g/cm^3). In contrast, compression test results for sampling group G3 show lower values compared

Fig. 2 Density profile of a healthy (a) and of a decayed stem wood (b). No resistance reduction occurred in a, in b the dark-brown stain perfectly corresponds to a resistance reduction



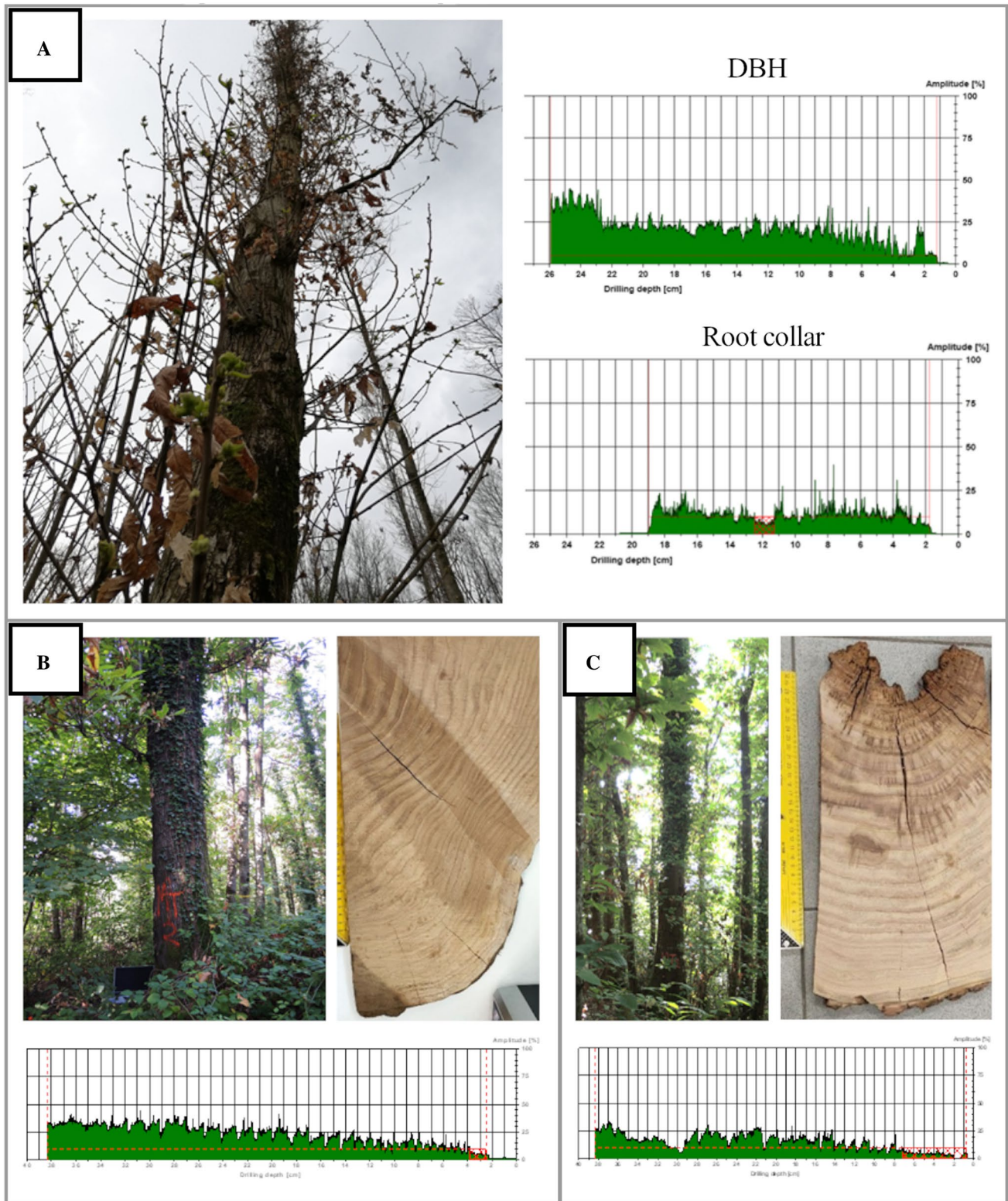


Fig. 3 Sample density profile of trees in the G2 and G3 groups. **a** In G2, only the suffering plants were selected (wood rot is indicated by epicormic branching). Sometimes the rot is not visible at the diameter at breast high (DBH) profile, but it is at the root collar. For

G3, a healthy tree (**b**) and one with decay (**c**) are shown. Epicormic branches are present in both samples, but in **c** its amount is higher than in **b**. The wood samples derive from the base of the trunk

Table 3 Amplitude of the profiles considered decayed and diameter of the damaged wood portion

Group	ID	Healthy wood [Amplitude (%)]	Decayed wood [Amplitude (%)]	Decayed diameter (%)
G1	G1–2	16.7 ± 6.9	5.5 ± 2.7	39.0
	G1–4	14.1 ± 6.3	5.8 ± 2.2	83.4
	G1–7	22.1 ± 5.9	15.4 ± 4.2	5.8
G2	G2–2a	33.9 ± 8.5	16.5 ± 2.4	5.2
	G2–2b	27.6 ± 8.1	16.7 ± 9.2	10.5
	G2–3a	24.6 ± 6.2	9.9 ± 4.4	2.1
G3	G3–1	19.4 ± 5.1	13.1 ± 4.4	87.5

Table 4 Physico-mechanical properties of the test samples (ρ_{12} ... density at 12% m.c., σ_{12} ... compressive strength parallel to the grain)

Group	ρ_{12} (g/cm ³)	σ_{12} (MPa)	Number of sampled trees	Number of tested samples
G1	0.621 ± 0.041	46.51 ± 5.46	6	68
G3	0.541 ± 0.042	29.65 ± 6.58	5	79

Table 5 Mean of each quartile sorting following highest specific density (* ρ_{12}) and highest compressive strength (* σ_{12}), respectively. Per each quartile, also the percentage of stained samples is reported

Group	Quartile	Mean * ρ_{12}	Stained samples (%)	Mean * σ_{12}	Stained samples (%)
G1	1	0.693 ± 0.019	42.9	54.38 ± 2.88	57.1
	2	0.647 ± 0.013	64.3	48.19 ± 0.93	57.1
	3	0.594 ± 0.008	37.5	46.18 ± 0.78	57.1
	4	0.547 ± 0.031	60.0	40.27 ± 4.65	33.3
G3	1	0.606 ± 0.024	42.1	39.05 ± 4.34	36.8
	2	0.555 ± 0.012	47.4	31.76 ± 0.88	42.1
	3	0.522 ± 0.006	31.6	27.72 ± 1.10	15.8
	4	0.472 ± 0.041	10.0	22.43 ± 3.12	35.0

to references, where values up to 50 MPa are reported (Romagnoli et al. 2014; Romagnoli and Spina 2013). The reason for such low values is not clear, although we need to consider that the disc samples from group G3 were obtained directly from the tree base, where tree rings are very wide (see Table 5-G3) and therefore lower values for mechanical test were shown already in past works of the authors (Romagnoli et al. 2014).

In Table 5, test samples based on ρ_{12} (mean * ρ_{12}) and then based on σ_{12} (mean * σ_{12}) were sorted. Even if in some cases stained samples are largely present in quartile with low values of ρ_{12} and σ_{12} , (Fig. 4a), there is no real trend between specific density, or compressive strength, with

coloured samples. In fact, some test samples with colour aberrations (Fig. 4b), had the highest value for specific gravity and compressive strength (Q1).

Figure 5 shows further information of the behaviour of the samples during mechanical testing. In Fig. 5a, the green pressure curve is from a specimen with sound wood, without colour alterations from the first quartile (Q1) of the compressive strength ranking in Table 5. The blue curve is related to a specimen with stained wood from the fourth quartile (Q4) of the ranking in Table 5. The first sample (G1-Q1, green line) has higher pressure resistance and lower deformation than the second sample (G1-Q4, blue line) and can deform up to 1 mm before breaking. In Fig. 5b, the situation is similar: sample G3-Q1 (sound wood, normal colour, high ρ_{12} and σ_{12}) and sample G3-Q4 (colour aberrations, and lower mechanical properties). In the case of G3, the pressure curves are more irregular than for G1. In both cases G1 and G3, the Q1 samples have higher resistance than Q4 samples.

Spectroscopic analysis (ATR-FTIR spectroscopy and imaging)

The chromatic aberrations in sound wood were analysed by ATR-FTIR spectroscopy focusing on dark areas in paratracheal and apotracheal zones, respectively. Furthermore, wood decay zones of Type-A and -B as identified by the macroscopic investigations (Fig. 1) were analysed. Bands assignments are reported in Table 6 according to Naumann et al. (2005), Özgenç et al. (2017) and Pandey and Pitman (2003). In Fig. 6, FTIR images based on the peak at 1030 cm⁻¹, which is referred to the C-O bond vibration in cellulose and hemicelluloses, are shown (Table 6).

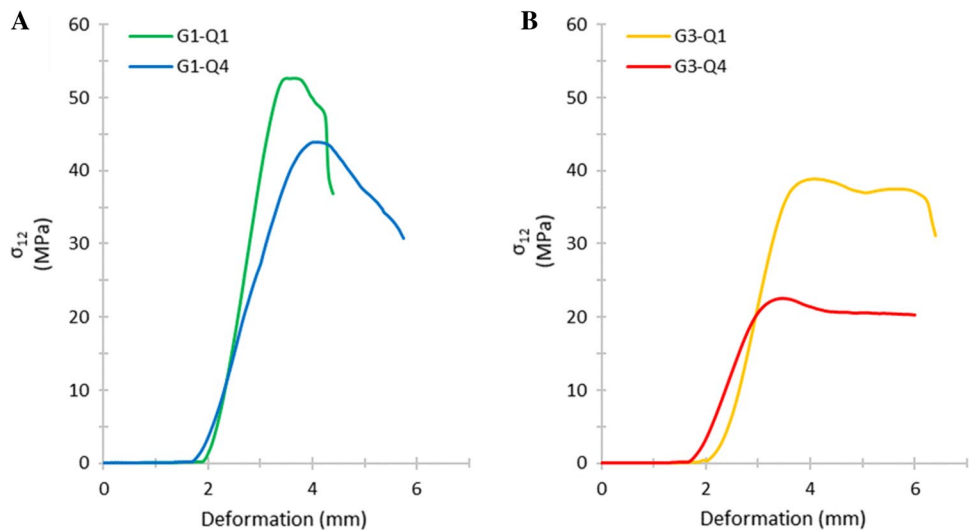
FTIR analysis shows differences in the identified zones with chromatic aberrations (Fig. 1) regarding the peak at 1030 cm⁻¹ related to cellulose. In the spectra related to the dark stains, both paratracheal and apotracheal, the absorbance of the bands shows some differences, which could be ascribed to a possible starting of wood decay. In general, the same absorbance bands are observed in the spectra of all investigated zones. However, band intensities are mostly lower especially the band at 1030 cm⁻¹ related to cellulose. Further, the band at 1230 cm⁻¹ is shifted slightly to lower wavenumbers in the spectra of the zones with colour aberrations. The spectrum of wood decayed by Type-A rot is much flatter with less intense bands indicating advanced degradation of both lignin and cellulose.

Additional information can be obtained from a semi-quantitative analysis of lignin- and carbohydrates-specific (cellulose and hemicellulose) absorbance bands intensities. In fact, comparing the different situations illustrated in Fig. 1, variations of the ratios indicate alterations of

Fig. 4 **a** Test samples from the fourth quartile (Q4) of both G1 and G3, with strong colour alteration. **b** Test samples from the first quartile (Q1) with high compressive strength with colour aberration as well



Fig. 5 Compressive strength parallel to grain. **a** Chart of the test samples of sampling group G1. Best sample (Q1) in green, and worst one (Q4) in blue. **b** Best sample (Q1) in yellow, and worst one (Q4) in red, both from sampling group G3



the abundances of the three wood components. The ratios were calculated using the equations (1) and (2) below:

$$L/C = \frac{\text{Abs}_{1505}}{\text{Abs}_{1030}} = \frac{\text{Lignin}}{\text{Cellulose}} \quad (1)$$

$$L/H = \frac{\text{Abs}_{1505}}{\text{Abs}_{1730}} = \frac{\text{Lignin}}{\text{Hemicellulose}} \quad (2)$$

where L/C is the ratio between the absorbance at 1505 cm^{-1} (Abs_{1505}), corresponding to lignin, and the absorbance at 1030 cm^{-1} (Abs_{1030}), corresponding to cellulose. L/H is the ratio between the Abs_{1505} and the absorbance at 1735 cm^{-1} (Abs_{1735}), corresponding to hemicellulose.

Results of the semiquantitative analysis are reported in Table 7. Colour abnormality attributed to Type-A wood rot supposedly is deriving from a white-rot fungus, since a decrease in the ratios L/C and L/H compared to sound wood is observed. Additionally, FTIR mapping of Type-A wood rot is shown in Fig. 7e, where a very irregular absorbance distribution is observed. Lignin degradation products deriving from white-rot decay can add absorbance in this range to the underlying C–O vibrations of carbohydrates. In contrast, in Type-B wood rot FTIR spectra, the ratios are higher than in the spectra of sound wood, meaning that cellulose and hemicellulose presence decreased relative to lignin as it generally occurs in brown-rot. Paratracheal strains show higher L/C and L/H ratios compared to sound wood, so they could be

Table 6 Wavenumber in the FTIR spectra and related bands assignment

Wavenumber (cm ⁻¹)	Peaks assignment
1750–1725	C=O stretch of acetyl and carbonyl groups in hemicellulose
1640	Not assigned
1608–1603	Aromatic skeletal and C=O stretch vibration in lignin
1510–1508	C=C stretching of aromatic skeletal vibration in lignin
1455–1421	C–H deformation in lignin and carbohydrates
1371–1369	C–H deformation in cellulose and hemicellulose, phenolic OH
1320	C–H vibration in cellulose and C–O vibration in syringyl derivatives
1250–1230	Syringyl ring and C–O stretching in lignin and xylan
1224	Syringyl ring and C–O stretching in lignin and xylan
1159–1155	C–O–C symmetric stretching in cellulose and hemicellulose
1105	C–O stretching (holocellulose)
1030	C–O vibration in cellulose and hemicellulose – CH deformation
897–893	C–H out of plane deformation in cellulose and hemicellulose In-plane symmetric vibrations of C–H in cellulose

associated to an incipient brown rot decay. In apotracheal stains zones, *L/C* ratio is lower than for sound wood, but *L/H* ratio is higher. Pandey and Pitman (2003) explain this last result as a selective (or preferential) white-rot decay with a preferred preliminary degradation of hemicellulose and lignin which later causes defibrillation through degradation of the middle lamella. Therefore, apotracheal stains might correspond to selective white-rot, where the only “not-touched” component is cellulose.

Morphological and anatomical analysis (SEM)

In Fig. 7, wood morphology of stained specimen are compared with sound wood using stereomicroscopy as well as SEM.

In sound wood (Fig. 7a), healthy cell walls as well as well-shaped tyloses are visible (Fig. 7b). One specimen characterized by the presence of both paratracheal (Fig. 7c, d) and apotracheal (Fig. 7e, f) stains show fungal hyphae inside the cells (Fig. 7d, f, g and h). Noteworthy, in the very dark-brown area in wood (Fig. 7e) the hyphae are widely abundant (Fig. 7f) and furthermore the tyloses are perforated by mycelium (Fig. 7d and h). Where dark apotracheal zones are present, the cell wall is thin (Fig. 7h) and fragile, in other specimen however the cell wall is still sound (Fig. 7r). In Type-A wood rot (Fig. 7i), fungi are present too (Fig. 7m and n). Furthermore, during the specimen preparation, the cells were compressed by the blade, indicating weakened cell walls (Fig. 7l). In Fig. 7m, at the top left side, the cell wall surface is rough and presenting a few cracks, while in the bottom right side the cell is more intact, as indicated by the integrity of the intervessel pits. As expected, in Type-B wood rot

(Fig. 7o, p) hyphae are present. In yellow areas (Fig. 7q) wood is sound, and there are encrusted extractives accumulations inside the tyloses (Fig. 7r).

Discussions

The study showed that chromatic aberrations are sometimes evidently related to decreasing mechanical properties which means a more or less advanced wood decay. We do not have scientific evidence on which pathogen could be responsible for the wood decay process or if it is the consequence of a parasitic attack on chestnut tree weakening tree defense. Chestnut forests and coppice stands are deliberately attacked by most widespread and known pathogens such as *Phytophthora* spp. (Peters et al. 2019), *Chryphonectria* spp. (Simoni et al. 2014), *Dryocosmus kuriphilus* (Clark et al. 2019; Marcolin et al. 2021; Peters et al. 2019). Thus, they can be sensitive to newly introduced pathogens such as *Gnomoniopsis smithogilvyi* (Gnomoniaceae, Diaporthales), which is well known for the white nut rot of chestnut and can presumably affect the gamic regeneration in forests. Furthermore, it was recently proven that this new agent induces symptoms similar to wood canker (Pasche et al. 2016; Shuttleworth and Guest 2017). The effects of pathogens on chestnut wood quality are less investigated. Gunduz et al. (2016) highlighted that in trees affected by chestnut blight disease, microscopic wood characteristics including vessel diameter, vessel frequency and vessel element length were irregular compared to healthy wood.

Several other pathogens have been associated with wood decay in chestnut such as *Capronia kleinmondensis* Marinc., M.J. Wingf. & Crous, *Collophora hispanica*

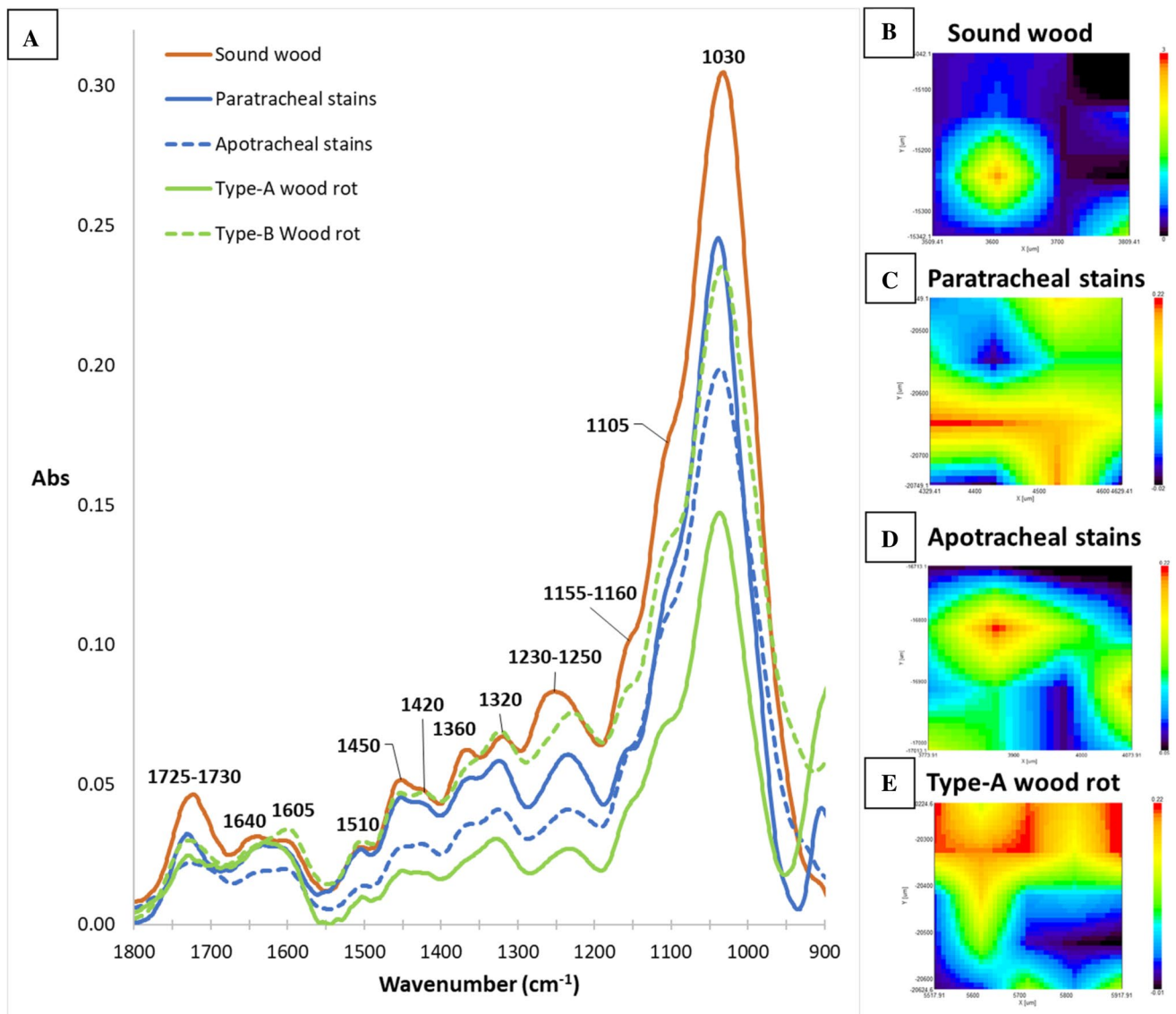


Fig. 6 ATR-FTIR spectra of the different analysed areas and related ATR-FTIR mapping for the wavenumber 1030 cm⁻¹. **a** A sound wood spectrum is compared with the spectra of paratracheal and apotra-

cheal stains as well as with zones with Type-A and -B wood rot. **b–e** ATR-FTIR mapped images for the wavenumber 1030 cm⁻¹ of the different stain types

D. Gramaje, *Moriostoma quercinum* B. Nordén, *Stereum hirsutum* (Willd.) Pers., *Phialocephala dimorphospora* W.B. Kendr. and *Fistulina hepatica* (Schaeff.) With. or

Schizophyllum commune Fr., *Serpula*, *Coniophora puteana* (Schumach.) P. Karst., just to mention some of the most found in heartwood causing lignin and cellulose degradation (Yurkewich et al. 2017). Some hypothesis come from FTIR analysis which even if it cannot detect the genus of the fungus (or fungi), it still delivers indications based on chestnut wood decay patches and the respective ratio of lignin and cellulose in the specific zones. Thus, based on the ratio of lignin and cellulose absorbance band intensities it is possible to distinguish between brown rot and white rot fungi causing the decay (Pandey and Pitman 2003).

Table 7 Ratios between lignin (1505 cm⁻¹) and cellulose (1030 cm⁻¹), respectively, hemicellulose (1735 cm⁻¹) absorbance bands

	Para-tracheal stains	Apotracheal stains	Type-A wood rot	Type-B wood rot	Sound wood
L/C	0.110	0.070	0.067	0.127	0.091
L/H	0.833	0.630	0.398	0.994	0.596

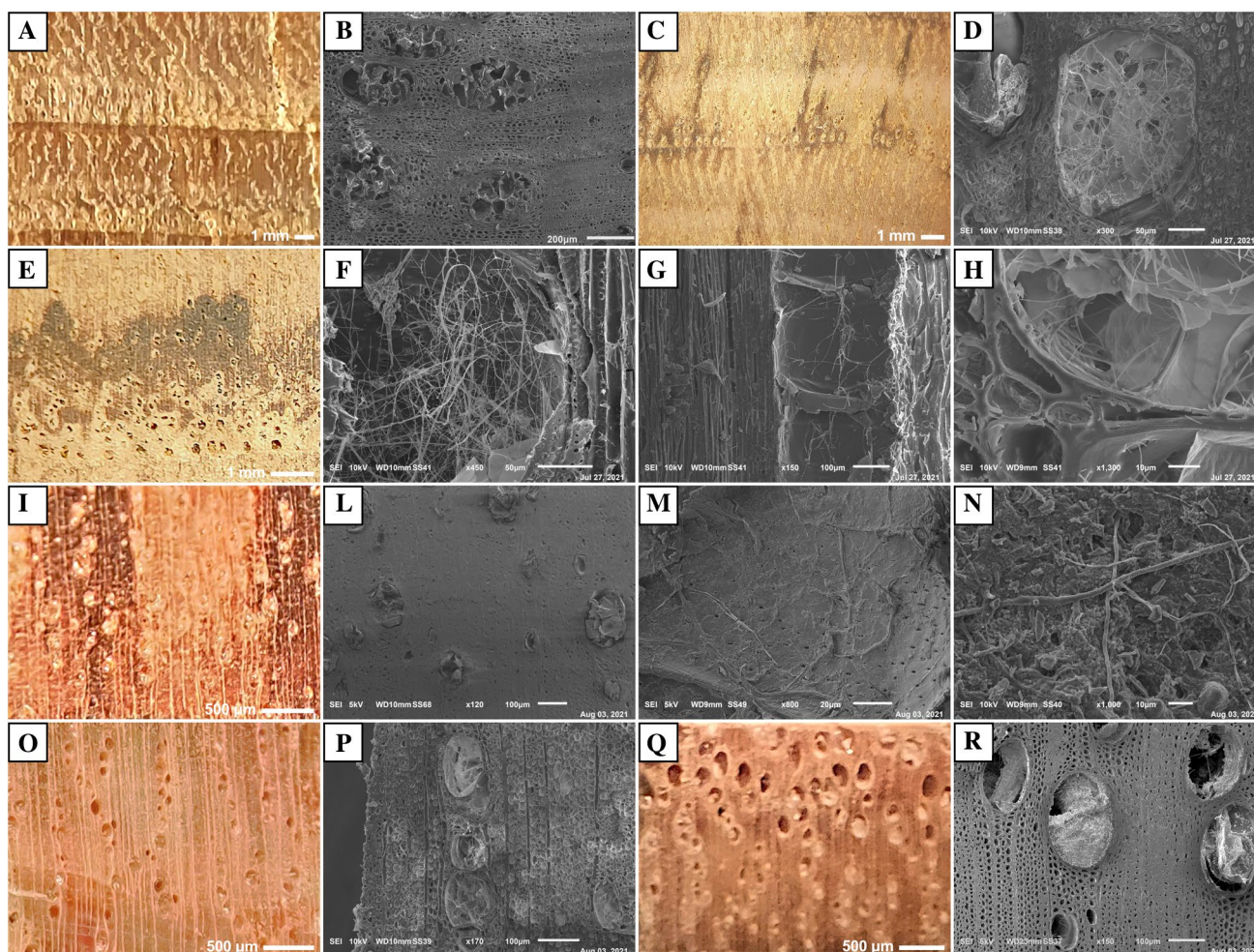


Fig. 7 **a** Sound wood in cross section. **b** Sound wood in cross section (SEM). **c** Paratracheal stains in cross section. **d** Paratracheal stains in cross section, perforated tyloses in vessel. **e** Apotracheal stains in cross section. **f** Apotracheal stains in radial section, stained area full of hyphae. **g** Apotracheal stains in radial section, regular coloured area with a slight amount of hyphae. **h** Apotracheal stains in cross section, perforated tyloses and damaged and thin vessel cell wall. **i** Type-B wood rot in cross section. **l** Type-B wood rot in cross sec-

tion, wood cells highly compressed. **m** Type-B wood rot in radial section, inner cell wall with encrusted deposits and hyphae. **n** Type-B wood rot in radial section, external surface completely damaged and particular of a hypha. **o** Type-A wood rot in cross section. **p** Type-A wood rot in cross section (SEM). **q** Yellow area in cross section. **r** Yellow area in cross section, well formed tyloses with extractives accumulations and present fungal hyphae

In the 1990s, a new heartwood discoloration, the Chestnut Red Stain (CRS), was noticed in Spain. Since 2006, the disease, locally referred to as Roig, became an economic concern for sweet chestnut farmers (Tusell and Rovira 2006). Wood industry does not accept diseased trees with stained wood and thus about 70% of timber value is currently lost (Regué et al. 2019). Among the nine fungal taxa isolated from CRS wood, *F. hepatica* was suggested to be the possible cause of the disease (Yurkewich et al. 2017). *F. hepatica* is a common pathogen that develops on several broadleaves. It is present in Europe, North America, South America, Australia and Asia (Butin 1995; Schwarze et al. 2000b). It can enter the tree trunk through mechanical damage and develop without appearing symptoms for

several years. *F. hepatica* attacks are enhanced by stress from environment and from stand conditions (Regué et al. 2019). Other chestnut rot pathogens like *C. hispanica* were recovered with high frequency from wood samples of other broadleaves showing necrosis and brown to black vascular streaking but never reported as the cause for discoloration of chestnut wood. At the end of our investigations it can be affirmed that chromatic aberrations found in Italian chestnut correspond to the CRS found in Spain even if in the Italian case the colour of the stain seems browner. In Italian chestnut, chromatic aberrations were found mainly in the lower portion of the tree in accordance with Yurkewich et al. (2017). There are some differences in the shape of the chromatic aberrations, as in the sampling group G1 a

darker but overall uniform heartwood colour was detected, while in sampling group G3, besides decay rot, there were irregularly stained patterns. In all examined samples, chromatic aberrations affected the density profiles obtained by IML RESI drilling as well as ATR-FTIR spectra and mapping. However, no obvious signs can associate chromatic aberrations with substantial losses of specific density (ρ) or axial compressive strength.

Although this study did not aim to detect the mycobiome associated to the stain patches, we could hypothesize that rot fungi are involved in the development of discolorations. The presence of discolouration within heartwood is often associated to a multitude of fungal enzyme phenol oxidases (laccase) and heme peroxidases, such as lignin peroxidase (LiP), manganese peroxidase (MnP) and versatile peroxidase (VP), produced by the fungi for lignin degradation (Schwarze et al. 2000a).

Our assumption is confirmed by the presence of rot symptoms and hyphae in all types of chromatic aberrations, as assessed by SEM analysis, in addition to IML-RESI drilling and ATR-FTIR spectroscopy, respectively. Moreover, chestnut wood rot fungi, especially *F. hepatica*, are commonly present in Latium region. The fungal attack has not yet compromised physical and mechanical properties like density and compressive strength of the wood. Thus, the presented results are consistent with the research of Schwarze et al. (2000a) and Yurkewich et al. (2017), who showed that wood attacked by *F. hepatica* is able to maintain mechanical properties for extended periods of time after colonization.

In the last century, climate changes and invasive alien species, mainly associated with the trade of plants (Santini et al. 2013), determined qualitative and quantitative changes in the chestnut ecosystem. This resulted in a general resilience decrease as well as changes in population dynamics and growth of some pathogens (e.g. *G. castanea*) (Vannini et al. 2017) and changes in the biological and disease cycle of primary chestnut pathogens like *C. parasitica* (Meyer et al. 2015).

In addition, forest harvesting can enhance the stress status of a forest. Practices that favour wounds on a tree for example by harvesting facilitate the entrance of wood decay agents (Wiedenbeck and Smith 2018) and cause ring shake defects in wood.

Furthermore, silvicultural management affects tree age and older trees are usually more sensitive to pathogens responsible of chromatic aberrations (Yurkewich et al. 2017). It was also suggested that the number of coppice rotations and the age of the existing root stock could be related to the presence of wood decay fungi in wood. Since we found the most damage in standard trees in the coppice, the result must be related to the actual discussion about the effective role of few and sparse standard trees in coppices, which is not considered anymore convenient from both an

economic as well as ecological point of view. The number of standard trees in coppices needs to be questioned regarding the higher potentiality of biotic attack caused by their presence (Manetti et al. 2017; Marini et al. 2021a; Roberts et al. 2020).

Since sampling was focused on trees with the most signs of suffering, no reliable conclusions can be made regarding incidence of chromatic aberrations in the population of the respective forest stands. Nevertheless, the investigation established a methodology to find an early decay stage in shoots and standards and it proved that chromatic aberrations are similar to red colour stain and are an indication for wood degradation. At the moment, they do not affect wood production in the investigated area and they do not affect the market although the symptoms cannot be neglected. Their presence would inevitably lead to an exclusive use of chestnut wood for energy use, which currently is the most widespread application in Italy especially for wood from coppice stands (Delfanti et al. 2014; Zambon et al. 2016) or wood of reduced quality (Paletto et al. 2019; Pieratti et al. 2019), compromising years of research that have valorised this species for uses with higher added value (Brunetti et al. 2020; Carbone et al. 2020).

Conclusions

New pest epidemics and diseases are emerging in forests world-wide. Many of them are novel associations between different pathogens, making its prediction and early detection challenging. Therefore, when an infection is registered, it is mostly already in a state of emergency. The phenomenon observed in our sampled trees, finds interesting correlations to the Spanish chestnut red stains, and even if we do not know what is the biotic agent, we can state that in our case the chromatic aberrations are associated with an early stage of wood decay, especially in the standards. Moreover, the discolourations were found at the plant collar and they have not affected the physical–mechanical properties in a significant way, in particular wood density. Optimization of forest management is crucial in order to limit the damage caused by pathogens and render the trees more resilient. At the moment, the incidence of the phenomenon is unknown, but it can be easily and early detected by the states of suffering of the plant and by means of IML-RESI drilling analysis. However, these findings suggest more attention and a deepening of the investigation to understand, which type of agent has caused the degradation, if and how climate change is responsible and how forestry activity can mitigate some effects. To keep the observed phenomenon under control is of profound interest in order to avoid to overlook premonitory signs of wood decay and tree mortality.

Acknowledgements We thank the municipality of Lariano (Rome), in particular Dott. Fabrizio Dezi for the support.

Authors' contributions Experimental plan MR. Data acquisition ST and SB. Results and Discussion all the authors. First draft MR and ST. Reviewing, checking and improving the manuscript GSM, LP, AMV and FZ. Final version checked by all the authors.

Funding The research was funded by the “Departments of Excellence—2018” Program (Dipartimenti di Eccellenza) of the Italian Ministry of Education, University and Research, DIBAF-Department of University of Tuscia, Project “Landscape 4.0—food, wellbeing and environment”. Further support was received by the project PON-MISE (“Imprese e Competitività”) F/2000 03/01-03/X45 “Innovazione e sostenibilità della filiera Foresta-Legno: bioeconomia circolare del legno e valorizzazione di foreste dell’Italia centro-meridionale”. The research was supported also by of Lariano municipality.

Declarations

Conflict of interest The authors declare that they have no conflicts of interests.

References

- Ayres MP, Lombardero MJ (2000). Assessing the consequences of global change for forest disturbance from herbivores and pathogens. *Sci Total Environ* 262(3):263–286. [https://doi.org/10.1016/S0048-9697\(00\)00528-3](https://doi.org/10.1016/S0048-9697(00)00528-3)
- Beccaro GL, Alma A, Bounous G, Gomes-Laranjo J (2019) The chestnut handbook: crop & forest management. CRC Press, Taylor & Francis Group, Boca Raton, FL (USA), p 378
- Blank L, Martín-García J, Bezos D, Vettraino AM, Krasnov H, Lomba JM, Fernández M, Diez JJ (2019) Factors affecting the distribution of pine pitch canker in Northern Spain. *Forests* 10(4):305. <https://www.mdpi.com/1999-4907/10/4/305>
- Bonsignore CP, Vizzari G, Vono G, Bernardo U (2020) Short-term cold stress affects parasitism on the Asian Chestnut Gall Wasp *Dryocosmus kuriphilus*. *Insects* 11(12):841. <https://doi.org/10.3390/insects11120841>
- Brunetti M, Nocetti M, Pizzo B, Aminti G, Cremonini C, Negro F, Zanuttini R, Romagnoli M, Scarascia Mugnozza G (2020) Structural products made of beech wood: quality assessment of the raw material. *Eur J Wood Wood Prod* 78(5):961–970. <https://doi.org/10.1007/s00107-020-01542-9>
- Buotte PC, Hicke JA, Preisler HK, Abatzoglou JT, Raffa KF, Logan JA (2017) Recent and future climate suitability for whitebark pine mortality from mountain pine beetles varies across the western US. *Forest Ecol Manage* 399:132–142. <https://doi.org/10.1016/j.foreco.2017.05.032>
- Butin H (1995) Tree diseases and disorders: causes, biology, and control in forest and amenity trees. Oxford University Press, 198 Madison Avenue, New York, NY 10016 (USA). <https://www.semanticscholar.org/paper/Tree-Diseases-and-Disorders%3A-Causes%2C-Biology%2C-and-Butin/38c84bad10d413197d3a5ee6dc9d0ffd05aa2ddd>
- Camarero JJ, Álvarez-Taboada F, Hevia A, Castedo-Dorado F (2018) Radial growth and wood density reflect the impacts and susceptibility to defoliation by gypsy moth and climate in radiata pine. *Front Plant Sci* 9(1582):12. <https://doi.org/10.3389/fpls.2018.01582>
- Carbone F, Moroni S, Mattioli W, Mazzocchi F, Romagnoli M, Portoghesi L (2020) Competitiveness and competitive advantages of chestnut timber laminated products. *Ann Forest Sci* 77(2):51. <https://doi.org/10.1007/s13595-020-00950-4>
- Clair B, Thibaut B (2014) Physical and mechanical properties of reaction wood. In: Gardiner B, Barnett J, Saranpää P, Gril J (eds) *The biology of reaction wood*. Springer Berlin Heidelberg, Berlin, Heidelberg, Germany, pp 171–200. https://doi.org/10.1007/978-3-642-10814-3_6
- Clark SL, Schlarbaum SE, Saxton AM, Baird R (2019) Eight-year blight (*Cryphonectria parasitica*) resistance of backcross-generation American chestnuts (*Castanea dentata*) planted in the south-eastern United States. *Forest Ecol Manage* 433:153–161. <https://doi.org/10.1016/j.foreco.2018.10.060>
- Conedera M, Tinner W, Krebs P, De Rigo D, Caudullo G (2016) *Castanea sativa* in Europe: distribution, habitat, usage and treats. In: San-Miguel-Ayaz J, De Rigo D, Caudullo G, Houston Durrant T, Mauri A (eds) *European Atlas of forest tree species*. Publication Office of the European Union, Luxemburg. <https://forest.jrc.ec.europa.eu/en/european-atlas/>
- Conedera M, Krebs P, Gehring E, Wunder J, Hülsmann L, Abegg M, Maringer J (2021) How future-proof is Sweet chestnut (*Castanea sativa*) in a global change context? *Forest Ecol Manage* 494:119320. <https://doi.org/10.1016/j.foreco.2021.119320>
- Costello LR, Quarles SL (1999). Detection of wood decay in blue gum and elm: an evaluation of the Resistograph and the portable drill. *J Arboricul* 25(6):311–318. <https://www.semanticscholar.org/paper/DETECTION-OF-WOOD-DECAY-IN-BLUE-GUM-AND-ELM%3A-AN-OF-Costello-Quarles/0f57fcbb785cdf67306ac9b992e061cf026bbc5c>
- Čufar K, Cherubini M, Gričar Ji, Prislan P, Spina S, Romagnoli M (2011) Xylem and phloem formation in chestnut (*Castanea sativa* Mill.) during the 2008 growing season. *Dendrochronologia* 29 (3):127–134. <https://doi.org/10.1016/j.dendro.2011.01.006>
- Delfanti LMP, Bedini R, Romagnoli M, Recanatesi F, Meacci F, Caruso L, Manzo A, Salvati L (2014) Estimation of agroforestry biomasses available for energy purposes in a municipality in central Italy as instrument for energy planning. *Appl Math Sci* 8(131):6577–6587. <https://doi.org/10.12988/ams.2014.46442>
- Ferracini C, Ferrari E, Pontini M, Saladini MA, Alma A (2019) Effectiveness of *Torymus sinensis*: a successful long-term control of the Asian chestnut gall wasp in Italy. *J Pest Sci* 92(1):353–359. <https://doi.org/10.1007/s10340-018-0989-6>
- Freitas TR, Santos JA, Silva AP, Fraga H (2021) Influence of climate change on chestnut trees: a review. *Plants* 10(7):1463. <https://doi.org/10.3390/plants10071463>
- Génova Fernández R, Gracia Alonso C (1984). Análisis dendroclimatólogico (*Castanea sativa* Mill) en el macizo del Montseny. Mediterránea. Serie de Estudios Biológicos 7:67–82. <https://doi.org/10.14198/MDTRRA1984.7.05>
- Greco S, Infusino M, Ienco A, Scalerio S (2018) How different management regimes of chestnut forests affect diversity and abundance of moth communities? *42(2):59–67*. <https://doi.org/10.12899/asr-1503>
- Gunduz G, Oral MA, Akyüz M, Aydemir D, Yaman B, Asik N, Bülbül AS, Allahverdiyev S (2016) Physical, morphological properties and Raman spectroscopy of Chestnut Blight Diseased *Castanea sativa* Mill. wood. *Cerne* 22:43–58. <https://doi.org/10.1590/01047760201622012101>
- Imposa S, Mele G, Corrao M, Coco G, Battaglia G (2014) Characterization of decay in the wooden roof of the S. Agata Church of Ragusa Ibla (Southeastern Sicily) by means of sonic tomography and resistograph penetration tests. *Int J Arch Herit* 8(2):213–223. <https://doi.org/10.1080/15583058.2012.685924>

- Johnstone D, Ades P, Moore G and Smith I (2007). Predicting wood decay in eucalypts using an expert System and the IML-resistograph drill. *Arboricultural Urban For* 33:76–82. <https://www.semanticscholar.org/paper/Predicting-wood-decay-in-eucalypts-using-an-expert-Johnstone-Ades/3a048a53556c06fbac7a1c678f311bffb9d82f5f#paper-header>
- Manetti MC, Becagli C, Carbone F, Corona P, Giannini T, Romano R, Pelleri F (2017) Linee guida per la selvicoltura dei cedui di castagno. Consiglio per la Ricerca in Agricoltura e l'Analisi dell'Economia Agraria (CREA), Rome, Italy. <https://www.reterurale.it/flex/cm/pages/ServeBLOB.php/L/IT/IDPagina/17415>
- Marcolin E, Pividori M, Colombari F, Manetti MC, Pelleri F, Conedera M, Gehring E (2021). Impact of the Asian gall wasp *Dryocosmus kuriphilus* on the radial growth of the European chestnut *Castanea sativa*. *J Appl Ecol* 58(6):1212–1224. <https://doi.org/10.1111/1365-2664.13861>
- Marini F, Battipaglia G, Manetti MC, Corona P, Romagnoli M (2019) Impact of climate, stand growth parameters, and management on isotopic composition of tree rings in chestnut coppices. *Forests* 10(12):1148. <https://doi.org/10.3390/f10121148>
- Marini F, Manetti MC, Corona P, Portoghesi L, Vinciguerra V, Tamantini S, Kuzminsky E, Zikeli F, Romagnoli M (2021a) Influence of forest stand characteristics on physical, mechanical properties and chemistry of chestnut wood. *Sci Rep* 11(1):1549. <https://doi.org/10.1038/s41598-020-80558-w>
- Marini F, Portoghesi L, Manetti MC, Salvati L, Romagnoli M (2021b) Gaps and perspectives for the improvement of the sweet chestnut forest-wood chain in Italy. *Ann Silvicult Res* 46(2):112–127. <https://doi.org/10.12899/asr-2203>
- Meyer JB, Gallien L, Prospero S (2015) Interaction between two invasive organisms on the European chestnut: does the chestnut blight fungus benefit from the presence of the gall wasp? *FEMS Microbiol Ecol* 91(11). <https://doi.org/10.1093/femsec/fiv122>
- Militz H, Busetto D, Hapla F (2003). Investigation on natural durability and sorption properties of Italian Chestnut (*Castanea sativa* Mill.) from coppice stands. *Holz als Roh- und Werkstoff* 61(2):133–141. <https://doi.org/10.1007/s00107-002-0357-2>
- Naumann A, Navarro-González M, Peddireddi S, Kües U, Polle A (2005) Fourier transform infrared microscopy and imaging: detection of fungi in wood. *Fungal Genetics Biol* 42(10):829–835. <https://doi.org/10.1016/j.fgb.2005.06.003>
- Nicolini E, Caraglio Y, Pélissier R, Leroy C, Roggy JC (2003) Epicormic Branches: a growth indicator for the tropical forest tree, *Dicorynia guianensis* Amshoff (Caesalpinaceae). *Ann Bot* 92(1):97–105. <https://doi.org/10.1093/aob/mcgl119>
- Özgenç Ö, Durmaz S, Kuştaş S (2017) Chemical analysis of tree barks using ATR-FTIR spectroscopy and conventional techniques. *BioResources* 12:9143–9151. <https://doi.org/10.15376/biores.12.4.9143-9151>
- Paletto A, Bernardi S, Pieratti E, Teston F, Romagnoli M (2019) Assessment of environmental impact of biomass power plants to increase the social acceptance of renewable energy technologies. *Heliyon* 5(7):e02070. <https://doi.org/10.1016/j.heliyon.2019.e02070>
- Palmeri V, Cascone P, Campolo O, Grande SB, Laudani F, Malacrino A, Guerrieri E (2014) Hymenoptera wasps associated with the Asian gall wasp of chestnut (*Dryocosmus kuriphilus*) in Calabria, Italy. *Phytoparasitica* 42(5):699–702. <https://doi.org/10.1007/s12600-014-0411-8>
- Pandey KK, Pitman A (2003) FTIR studies of the changes in wood chemistry following decay by brown-rot and white-rot fungi. *Int Biodeterior Biodegrad* 52:151–160. [https://doi.org/10.1016/S0964-8305\(03\)00052-0](https://doi.org/10.1016/S0964-8305(03)00052-0)
- Pasche S, Calmin G, Auderset G, Crovadore J, Pelleteret P, Mauch-Mani B, Barja F, Paul B, Jermini M, Lefort F (2016). *Gnomoniopsis smithogilyvi* causes chestnut canker symptoms in *Castanea sativa* shoots in Switzerland. *Fungal Genetics Biol* 87:9–21. <https://doi.org/10.1016/j.fgb.2016.01.002>
- Peters FS, Wunderlich L, Metzler B (2019) First report of *Phytophthora cinnamomi* in forest stands in Germany. *Forest Pathology* 49(2):e12485. <https://doi.org/10.1111/efp.12485>
- Pieratti E, Bernardi S, Romagnoli M, Sartori O, Paletto A (2019) Offerta e domanda di biomasse legnose ad uso energetico in provincia di Trento: un'indagine conoscitiva. *Forest@ Rivista di Selvicoltura ed Ecologia Forestale* 16(2):16–25. <https://doi.org/10.3832/efor3037-016>
- Pureswaran DS, Roques A, Battisti A (2018) Forest insects and climate change. *Curr for Rep* 4(2):35–50. <https://doi.org/10.1007/s40725-018-0075-6>
- Regué A, Bassié L, De-Miguel S, Colinas C (2019) Environmental and stand conditions related to *Fistulina hepatica* heart rot attack on *Castanea sativa*. *Forest Pathol* 49(3):e12517. <https://doi.org/10.1111/efp.12517>
- Rigling D, Prospero S (2018) *Cryphonectria parasitica*, the causal agent of chestnut blight: invasion history, population biology and disease control. *Mol Plant Pathol* 19(1):7–20. <https://doi.org/10.1111/mpp.12542>
- Roberts M, Gilligan CA, Kleczkowski A, Hanley N, Whalley AE, Healey JR (2020) The effect of forest management options on forest resilience to pathogens. *Front Forests Global Change* 3(7). <https://doi.org/10.3389/ffgc.2020.00007>
- Romagnoli M, Nocetti M, Sarlato M, Evangelista L (2004) Dendrochronological assessment of chestnut (*Castanea sativa* Mill.) for dating purposes in Central Italy. *Dendrochronologia* 21(3):117–130. <https://doi.org/10.1078/1125.7865.00048>
- Romagnoli M, Cherubini M, Prislán P, Gričar J, Spina S, Čufar K (2011) Main phases of wood formation in chestnut (*Castanea sativa*) in Central Italy—comparison of seasons 2008 and 2009. *Drvna Industrija* 62(4):269–275. <https://hrcak.srce.hr/75153>
- Romagnoli M, Spina S (2013) Physical and mechanical wood properties of ring-shaken chestnut (*Castanea sativa*) trees. *Can J Forest Res* 43:200–207. <https://doi.org/10.1139/cjfr-2012-0357>
- Romagnoli M, Cavalli D, Spina S (2014) Wood quality of chestnut: relationship between ring width, specific gravity, and physical and mechanical properties. *BioResources* 9(1). <https://doi.org/10.15376/biores.9.1.1132-1147>
- Romagnoli M, Cavalli D, Pernarella R, Zanuttini R, Togni M (2015) Physical and mechanical characteristics of poor-quality wood after heat treatment. *iForest Biogeosci For* 8:884–891. <https://doi.org/10.3832/ifer1229-007>
- Santini A, Ghelardini L, De Pace C, Desprez-Loustau ML, Capretti P, Chandelier A, Cech T, Chira D, Diamandis S, Gaitniekis T, Hantula J, Holdenrieder O, Jankovsky L, Jung T, Jurc D, Kirisits T, Kunca A, Lygis V, Malecka M, Marcais B, Schmitz S, Schumacher J, Solheim H, Solla A, Szabó I, Tsopeles P, Vannini A, Vettraino AM, Webber J, Woodward S, Stenlid J (2013) Biogeographical patterns and determinants of invasion by forest pathogens in Europe. *New Phytol* 197(1):238–250. <https://doi.org/10.1111/j.1469-8137.2012.04364.x>
- Sartori C, Dini F, Torello Marinoni D, Mellano MG, Beccaro GL, Alma A, Quacchia A, Botta R (2015) Impact of the Asian wasp *Dryocosmus kuriphilus* (Yasumatsu) on cultivated chestnut: Yield loss and cultivar susceptibility. *Sci Hortic* 197:454–460. <https://doi.org/10.1016/j.scienta.2015.10.004>
- Schwarze FWMR, Baum S and Fink S (2000a) Dual modes of degradation by *Fistulina hepatica* in xylem cell walls of *Quercus robur*. *Mycol Res* 104(7):846–852. <https://doi.org/10.1017/S0953756299002063>
- Schwarze FWMR, Engels J, Mattheck C (2000b) Fungal strategies of wood decay in trees. Springer, Berlin, Heidelberg. <https://doi.org/10.1007/978-3-642-57302-6>

- Seybold SJ, Klingeman WE III, Hishinuma SM, Coleman TW, Graves AD (2019) Status and impact of Walnut Twig beetle in urban forest, orchard, and native forest ecosystems. *J For* 117(2):152–163. <https://doi.org/10.1093/jofore/fvy081>
- Shuttleworth LA, Guest DI (2017) The infection process of chestnut rot, an important disease caused by *Gnomoniopsis smithogilvyi* (Gnomoniaceae, Diaporthales) in Oceania and Europe. *Austr Plant Pathol* 46(5):397–405. <https://doi.org/10.1007/s13313-017-0502-3>
- Simoni S, Nannelli R, Roversi PF, Turchetti T, Bouneb M (2014) *Thyrophagus corticalis* as a vector of hypovirulence in *Cryphonectria parasitica* in chestnut stands. *Exp Appl Acarol* 62(3):363–375. <https://doi.org/10.1007/s10493-013-9738-y>
- Spina S, Romagnoli M (2010) Characterization of ring shake defect in chestnut (*Castanea sativa* Mill.) wood in the Lazio Region (Italy). *For Int J Forest Res* 83(3):315–327. <https://doi.org/10.1093/forestry/cpq014>
- Thurman JH, Crowder DW, Northfield TD (2017) Biological control agents in the Anthropocene: current risks and future options. *Curr Opin Insect Sci* 23:59–64. <https://doi.org/10.1016/j.cois.2017.07.006>
- Tusell LM, Rovira N (2006). La situació actual del castanyer (*Castanea sativa*) a Catalunya. Consorci Forestal de Catalunya
- Ugolini F, Massetti L, Pedrazzoli F, Tognetti R, Vecchione A, Zulini L, Maresi G (2014) Ecophysiological responses and vulnerability to other pathologies in European chestnut coppices, heavily infested by the Asian chestnut gall wasp. *Forest Ecol Manage* 314:38–49. <https://doi.org/10.1016/j.foreco.2013.11.031>
- UNI ISO 3787:1985 (1985) Wood. Test methods. Determination of ultimate stress in compression parallel to grain. Italian Unification Body (UNI), Milan, Italy, pp 1–4
- Vannini A, Morales-Rodriguez C, Aleandri MP, Bruni N, Dalla Valle M, Mazzetto T, Martignoni D, Vettraino AM (2018). Emerging new crown symptoms on *Castanea sativa* (Mill.): attempting to model interactions among pests and fungal pathogens. *Fungal Biol* 122(9):911–917. <https://doi.org/10.1016/j.funbio.2018.05.006>
- Vannini A, Vettraino AM, Martignoni D, Morales-Rodriguez C, Contarini M, Caccia R, Paparatti B, Speranza S (2017) Does *Gnomoniopsis castanea* contribute to the natural biological control of chestnut gall wasp? *Fungal Biol* 121(1):44–52. <https://doi.org/10.1016/j.funbio.2016.08.013>
- Vettraino AM, Morel O, Perlerou C, Robin C, Diamandis S, Vannini A (2005) Occurrence and distribution of *Phytophthora* species in European chestnut stands, and their association with Ink Disease and crown decline. *Eur J Plant Pathol* 111(2):169. <https://doi.org/10.1007/s10658-004-1882-0>
- Wiedenbeck J, Smith K (2018) Hardwood management, tree wound response, and wood product value. *For Chronicle* 94:292–306. <https://doi.org/10.5558/tfc2018-042>
- Yurkewich JI, Castaño C, Colinas C (2017) Chestnut red stain: identification of the fungi associated with the costly discoloration of *Castanea sativa*. *Forest Pathol* 47. <https://doi.org/10.1111/efp.12335>
- Zambon I, Monarca D, Cecchini M, Bedini R, Longo B, Romagnoli M, Marucci A (2016) Alternative energy and the development of local rural contexts: an approach to improve the degree of smart cities in the Central-Southern Italy. *Contemp Eng Sci* 9(28):1371–1386. <https://doi.org/10.12988/ces.2016.68143>

Publisher's Note Springer Nature remains neutral with regard to jurisdictional claims in published maps and institutional affiliations.